Acta Crystallographica Section B
Structural Science
ISSN 0108-7681

The elusive $[Ni(H_2O)_2(15\text{-crown-}5)]^{2+}$ cation and related co-crystals of nickel(II) hydrates and 15-crown-5

Maxime A. Siegler, Sean Parkin, John P. Selegue and Carolyn Pratt Brock*

Department of Chemistry, University of Kentucky, Lexington, KY 40506-0055, USA

Correspondence e-mail: cpbrock@uky.edu

Received 1 July 2008
Accepted 17 October 2008

Initial attempts to make $[Ni(H_2O)_2(15\text{-crown-}5)](NO_3)_2$, *i.e.* to insert the Ni^{2+} ion into the 15-crown-5 macrocycle, gave the mono- (two polymorphs) and dihydrate of a co-crystal of $[Ni(H_2O)_6](NO_3)_2$ and 15-crown-5 (1,4,7,10,13-pentaoxacyclopentadecane = 15C5). Synthetic routes designed to restrict the water available to the Ni^{2+} cation gave three additional compounds, $[Ni(H_2O)_6](NO_3)_2$-*trans*-$[Ni(H_2O)_4(MeOH)_2](NO_3)_2$·2(15C5), *cis*-$[Ni(H_2O)_4(NO_3)_2]$-*trans*-$[Ni(H_2O)_4(NO_3)_2]$·2(15C5) and $[Ni(H_2O)_2(MeCN)(NO_3)_2]$·15C5·MeCN. All five compounds contain Ni^{2+} ions with two *trans* aqua ligands. In all six structures these aqua ligands make hydrogen bonds to the 15C5 molecules to form stacks in which the Ni complexes and 15C5 molecules alternate. The structures are surprisingly complicated: all are co-crystals, some are also solvates, and most have $Z' > 1$. The target compound was finally prepared by heating pale green crystals of $[Ni(H_2O)_6](NO_3)_2$·15C5·$2H_2O$ to over 350 K and then cooling the resulting mixture of yellow crystals and solution to room temperature. Formation of the target compound seems to be favored at higher temperatures by a positive $\Delta_{rxn}S^o$ and an increased rate of ligand exchange.

1. Introduction

Structures of two phases each of the six compounds $[M(H_2O)_2(15\text{-crown-}5)](NO_3)_2$ (M = Mg, Mn, Fe, Co, Cu and Zn; 15-crown-5 = 1,4,7,10,13-pentaoxacyclopentadecane = 15C5) have been studied previously (Hao, Parkin & Brock, 2005; Hao, Siegler *et al.*, 2005; Siegler, Hao *et al.*, 2008*a*). The structures are all very closely related. In all cases the divalent metal ion is located inside the crown ether. The five ether O atoms are approximately coplanar and the five $M—O_{ether}$ distances are approximately equal.

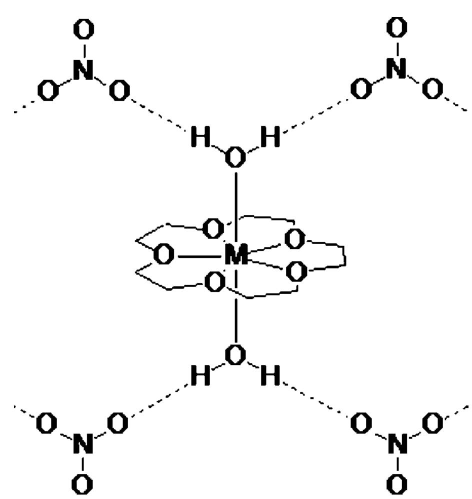

There is a gap in this series at M = Ni. Tables of effective ionic radii (Shannon, 1976; Greenwood & Earnshaw, 1997) suggested that a Ni^{2+} ion should fit inside the crown, but we found little precedent for such coordination. A survey of version 5.29 (November 2007 plus January 2008 update) of the Cambridge Structural Database (Allen, 2002; hereafter the CSD) located coordinates for four structures (refcodes XEMGAX, XEMGEB, XEMGIF, XEMGOL; Steed *et al.*, 2001) containing Ni^{2+}, 15-crown-5, water and a simple counterion (NO_3^-, Br^- or ClO_4^-), but the Ni^{2+} ion is not coordinated by the macrocycle in any of them. One entry {BIHFED; $[Ni(EtOH)_2(15C5)](PF_6)_2$; Simonsen *et al.*, 1982} does show a diagram with a Ni^{2+} ion located inside the crown, but the reference is to a conference abstract, no coordinates are archived, R = 0.091, and it seems that no full structure report was ever published.

We therefore decided to try to make the compound $[Ni(H_2O)_2(15C5)](NO_3)_2$. Before we were finally successful we had made five other compounds that all contained a six-coordinate Ni^{2+} ion (with at least two of the ligands being water molecules), nitrate ions and a 15-crown-5. The structure of one of these compounds (refcode XEMGIF) had been reported by Steed *et al.* (2001), but the other four are new. The five compounds have water/Ni^{2+} ratios as high as 8 and as low as 2. In none of them is the Ni^{2+} ion coordinated by the crown ether. All five compounds should therefore be considered to be co-crystals, and in some cases solvated co-crystals, of a nitrate salt of a six-coordinate Ni^{2+} ion. A list of all compounds is given in Table 1.

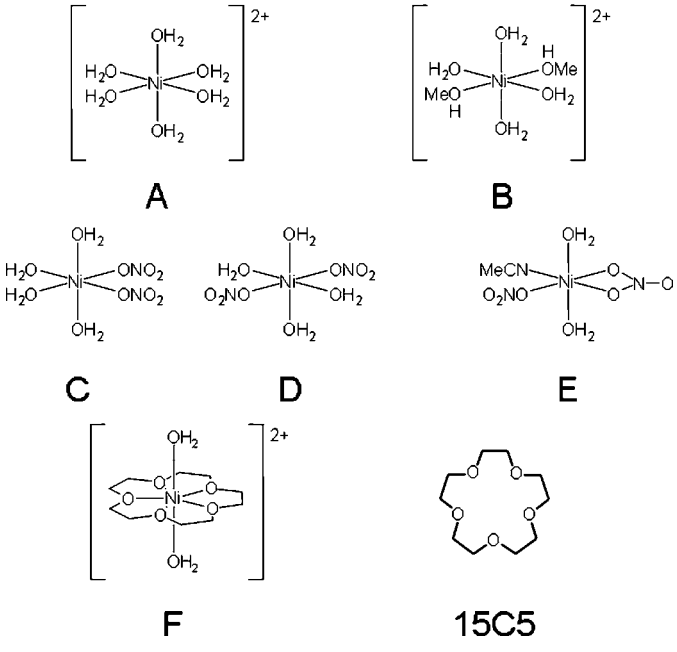

Crystals of the target compound were eventually obtained by heating the pale green crystals of $[Ni(H_2O)_6](NO_3)_2{\cdot}15C5{\cdot}2H_2O$ to 373 K, holding the resulting mixture of crystals and solution at that temperature for 5–10 min, and then cooling to room temperature. Subsequent experiments suggested heating to over 350 K would have been sufficient.

Table 1
List of structures.

The capital letters A–F refer to the nickel complexes shown in the scheme.

ID	Compound formula	No. of different constituents	Z' at 90 K	Ratio of H_2O to Ni^{2+}
(1)	$[Ni(H_2O)_6](NO_3)_2{\cdot}$15-crown-5$\cdot 2H_2O$ **[A(NO$_3$)$_2$·15C5·2H$_2$O]**	3	1	8:1
(2*a*)	$[Ni(H_2O)_6](NO_3)_2{\cdot}$15-crown-5$\cdot H_2O$ **[A(NO$_3$)$_2$·15C5·H$_2$O**; first polymorph]	3	2	7:1
(2*b*)	$[Ni(H_2O)_6](NO_3)_2{\cdot}$15-crown-5$\cdot H_2O$ **[A(NO$_3$)$_2$·15C5·H$_2$O**; second polymorph]	3	3	7:1
(3)	$[Ni(H_2O)_6](NO_3)_2$-*trans*-$[Ni(H_2O)_4(MeOH)_2](NO_3)_2$-2(15-crown-5) **[A(NO$_3$)$_2$·B(NO$_3$)$_2$·2(15C5)]**	3	$\frac{1}{2}$	5:1
(4)	*cis*-$[Ni(H_2O)_4(NO_3)_2]$-*trans*-$[Ni(H_2O)_4(NO_3)_2]{\cdot}$2(15-crown-5) **[C·D·2(15C5)]**	3	1	4:1
(5)	$[Ni(H_2O)_2(MeCN)(NO_3)_2]{\cdot}$(15-crown-5) MeCN **[E·15C5·MeCN]**	3	2	2:1
(6)	$[Ni(H_2O)_2$(15-crown-5)$](NO_3)_2$ **[F(NO$_3$)$_2$]**	1	3	2:1

Seven structures are reported here because two polymorphs were discovered for one of the six compounds. The structure XEMGIF is included because the original determination (Steed *et al.*, 2001) was at 173 K and we wanted to be able to make comparisons at 90 K.

All the structures reported are unusual in having asymmetric units that are considerably larger than expected. Six of the seven structures are co-crystals that contain three different chemical components (metal complexes, 15C5 and, in some cases, solvent molecules). In two of those six there are two Ni-containing cations that are either isomers or that have different sets of ligands. Four of the seven structures have Z' = 2 or 3, *i.e.* have two or three independent formula units in the asymmetric unit. Steed *et al.* (2001) noted the surprising frequency of large asymmetric units in co-crystals of 15C5 and simple metal complexes.

Even the existence of a large number of compounds that are co-crystals of a simple metal complex and 15C5 is a surprise. Since fractional crystallization is the norm, and since the ionic interactions and hydrogen bonds in hydrated metal salts are strong, the inclusion of the 15C5 molecule is unexpected. Ether O atoms are not thought of as particularly good hydrogen-bond acceptors compared with water, but two *trans* aqua ligands of five nickel complexes each form O—H···O bonds to included 15C5 molecules. The reasons for the prevalence of the $15C5{\cdots}H_2O{-}M{-}OH_2{\cdots}15C5{\cdots}H_2O{-}M{-}OH_2$ 'synthon' are explored.

The difficulty in getting the Ni^{2+} ion inside the 15C5 ligand seems to be a consequence of the ion's size and electron configuration. The target compound was probably obtained because at the higher temperature the entropy increase associated with replacing four aqua ligands with one crown ligand became determining and because the rate of ligand exchange became faster.

Finally, four of these six compounds were found to undergo at least one phase transition between room temperature and 90 K without any significant degradation of the quality of the diffraction pattern (Siegler, 2007). For each of two compounds three phase transitions were found. Studies of these phase sequences will be reported separately (Siegler, Hao *et al.*, 2008*b*; Siegler, Parkin & Brock, 2008).

2. Experimental

2.1. Syntheses

The compound $[Ni(H_2O)_2(15C5)](NO_3)_2$ could not be made by the procedure used to give $[M(H_2O)_2(15C5)](NO_3)_2$, M = Mg, Mn, Co, Cu and Zn (Hao, Parkin & Brock, 2005; Hao, Siegler *et al.*, 2005). Crystals of those non-Ni compounds were all grown by slow evaporation at room temperature of aqueous solutions that were equimolar in $M(NO_3)_2{\cdot}nH_2O$ and 15C5. The procedure for the M = Fe compound was a little more complicated because it involved *in situ* reduction of $Fe^{III}(NO_3)_3{\cdot}9H_2O$ with Fe powder in 3*M* HNO_3.

Evaporation of aqueous solutions equimolar in $Ni(NO_3)_2{\cdot}6H_2O$ and 15-crown-5 invariably gave the compound $[Ni(H_2O)_6](NO_3)_2{\cdot}15C5{\cdot}2H_2O$ (see Steed *et al.*, 2001). Attempts were then made to restrict the water available to the Ni^{2+} ion, usually by recrystallizing from nonaqueous solvents. A series of compounds in which the ratio of water molecules to Ni^{2+} ions decreased from a high of 8:1 to a low of 2:1 was prepared, but the Ni^{2+} ion still remained outside the crown. As the ratio of water to the Ni^{2+} ion is lowered the equatorial aqua ligands are replaced by methanol, nitrato and acetonitrile ligands. The target compound was finally prepared by heating crystals of $[Ni(H_2O)_6](NO_3)_2{\cdot}15C5{\cdot}2H_2O$ to over 370 K (350 K would probably have been sufficient) and then allowing the resulting mixture of yellow crystals and a small amount of solution to cool.

All crystallizations described below were carried out at room temperature over a period of hours to days unless otherwise stated. The nickel nitrate salt used was the hexahydrate. Compound identity was established by the structure determination. Crystallization dishes were examined under the microscope to look for obvious signs that more than one solid phase was present.

2.1.1. $[Ni(H_2O)_6](NO_3)_2{\cdot}$15-crown-5$\cdot 2H_2O$ [the dihydrate, (1), hexaaquanickel(II) nitrate–1,4,7,10,13-pentaoxacyclopentadecane (hereafter 15-crown-5)–water (1/1/2)]. Pale green crystals of the dihydrate grew as laths that are very long in the **c** direction, which is the direction of the $15C5\cdots H_2O-M-OH_2\cdots 15C5$ chain. The bounding faces that are perpendicular to **c** belong to the form {110}. There was no evidence of any other product. A picture of several typical crystals is given in Fig. S-1 of the supplementary material.[1]

2.1.2. $[Ni(H_2O)_6](NO_3)_2{\cdot}$(15-crown-5)$\cdot H_2O$ [the monohydrate, polymorphs (2*a*) and (2*b*), hexaaquanickel(II) nitrate–15-crown-5–water (1/1/1)]. Pale green crystals of the first polymorph (2*a*) of the monohydrate were grown from acetone, methanol and ethanol solutions. Crystals grow as tablets that are longest in the **a** direction (the chain direction); important faces are {010} and {001}. A picture showing several typical crystals is given in Fig. S-2 of the supplementary material. Under the microscope the monohydrate crystals can be distinguished easily from the dihydrate crystals, which are much longer and thinner.

Pale green crystals of the second polymorph (2*b*) were obtained from crystals of the compound $[Ni(H_2O)_6](NO_3)_2{\cdot}15C5{\cdot}2H_2O$ by heating. If crystals of the dihydrate were heated to 348 K and then cooled over a period of *ca* 20 min to room temperature macroscopic crystals of (2*b*) were sometimes obtained. Crystal quality was not, however, very good, and the procedure sometimes gave a mixture of phases.

2.1.3. $[Ni(H_2O)_6](NO_3)_2$-*trans*-$[Ni(H_2O)_4(MeOH)_2](NO_3)_2$-2(15-crown-5) [the methanol compound, (3), hexaaquanickel(II) nitrate–*trans*-tetraaquadimethanolnickel(II) nitrate–15-crown-5 (1/1/2)]. Pale green crystals of the methanol compound were originally grown by refluxing an acetone/2,2-DMP (2,2-DMP = 2,2-dimethoxypropane) solution equimolar in $Ni(NO_3)_2{\cdot}6H_2O$ and 15C5. The 2,2-DMP was added to scavenge water. Crystal quality was unsatisfactory. Later we discovered that much better crystals of this compound could be grown by evaporation of a methanol solution containing nickel nitrate hexahydrate and 15C5. Crystals of (3) grew as irregular blocks that could be distinguished easily from the tablets of (2*a*) that grew from the same solution.

2.1.4. *cis*-$[Ni(H_2O)_4(NO_3)_2]$-*trans*-$[Ni(H_2O)_4(NO_3)_2]{\cdot}$2(15-crown-5) [the *cis*/*trans* compound, (4), *cis*-tetraaquadinitratonickel(II)–*trans*-tetraaquadinitratonickel(II)–15-crown-5 (1/1/2)]. Pale green crystals of the *cis*/*trans* compound grew along with crystals of (2*a*) from acetone solutions. Crystals of this co-crystal of *cis* and *trans* isomers were also obtained from 2-butanol and tetrahydrofuran solutions. Crystals grown from acetone were plates thinnest along **b** that could be distinguished by their thickness from crystals of the first monohydrate polymorph (2*a*) that grew from the same solution. A picture showing a typical crystal of the *cis*/*trans* compound is given in Fig. S-3 of the supplementary material. Crystals of (4) grown from other solvents were more equidimensional.

When the solvent was acetone crystals of the *cis*/*trans* compound (4) grew first and near the top of the vial; crystals of the first monohydrate polymorph (2*a*) grew later and at the bottom of the vial.

2.1.5. $[Ni(H_2O)_2(MeCN)(NO_3)_2]{\cdot}$(15-crown-5)$\cdot$MeCN [the acetonitrile compound, (5), acetonitrilediaquadinitratonickel(II)–15-crown-5–acetonitrile (1/1/1)]. Pale green crystals of the acetonitrile compound were grown from acetonitrile solutions. Only some of the evaporation containers produced crystals of satisfactory quality. It proved difficult to reproduce the original results. Evaporation of acetonitrile solutions sometimes produced crystals of the first polymorph of the

[1] Supplementary data for this paper are available from the IUCr electronic archives (Reference: BS5068). Services for accessing these data are described at the back of the journal.

Table 2
Experimental data.

	(1)	(2*a*)	(2*b*)	(3)
Crystal data				
Chemical formula	$C_{10}H_{20}O_5{\cdot}H_{12}NiO_6^{2+}{\cdot}2NO_3^{1-}{\cdot}2H_2O$	$C_{10}H_{20}O_5{\cdot}H_{12}NiO_6^{2+}{\cdot}2NO_3^{1-}{\cdot}H_2O$	$C_{10}H_{20}O_5{\cdot}H_{12}NiO_6^{2+}{\cdot}2NO_3^{1-}{\cdot}H_2O$	$C_{10}H_{20}O_5{\cdot}C_2H_{16}NiO_6{\cdot}2NO_3{\cdot}C_{10}H_{20}O_5{\cdot}H_{12}NiO_6{\cdot}2NO_3$
M_r	547.12	529.10	529.10	1050.22
Cell setting, space group	Monoclinic, $P2_1/c$	Monoclinic, $B2_1$	Triclinic, $P\overline{1}$	Monoclinic, $P2_1/n$
Temperature (K)	90.0 (2)	90.0 (2)	90.0 (2)	90.0 (2)
a, b, c (Å)	11.950 (1), 12.686 (1), 15.988 (1)	16.176 (2), 16.514 (2), 17.876 (2)	16.036 (1), 24.765 (2), 10.163 (1)	16.241 (1), 15.481 (1), 10.429 (1)
α, β, γ (°)	90.00, 101.51 (1), 90.00	90.00, 106.42 (1), 90.00	89.71 (1), 122.53 (1), 83.58 (1)	90.00, 120.75 (1), 90.00
V (Å^3)	2375.0 (3)	4580.5 (10)	3371.2 (6)	2253.5 (4)
Z	4	8	6	2
D_x (Mg m^{-3})	1.530	1.535	1.564	1.548
Radiation type	Mo $K\alpha$	Mo $K\alpha$	Mo $K\alpha$	Mo $K\alpha$
μ (mm^{-1})	0.90	0.93	0.95	0.94
Crystal form, color	Parallelepiped, pale green	Parallelepiped, pale green	Irregular block, pale green	Irregular block, pale green
Crystal size (mm)	0.30 × 0.25 × 0.20	0.40 × 0.20 × 0.20	0.20 × 0.15 × 0.10	0.20 × 0.15 × 0.11
Data collection				
Diffractometer	Nonius KappaCCD	Nonius KappaCCD	Nonius KappaCCD	Nonius KappaCCD
Data collection method	ω scans at fixed $\chi = 55°$	ω scans at fixed $\chi = 55°$	ω scans at fixed $\chi = 55°$	ω scans at fixed $\chi = 55°$
Absorption correction	Multi-scan†	Multi-scan†	Multi-scan†	Multi-scan†
T_{min}	0.773	0.707	0.833	0.834
T_{max}	0.840	0.836	0.911	0.903
No. of measured, independent and observed reflections	40 317, 5463, 3979	43 409, 10 301, 8534	39 170, 15 437, 8504	36 203, 5174, 3430
Criterion for observed reflections	$I > 2\sigma(I)$	$I > 2\sigma(I)$	$I > 2\sigma(I)$	$I > 2\sigma(I)$
R_{int}	0.061	0.041	0.103	0.057
θ_{max} (°)	27.5	27.5	27.5	27.5
Refinement				
Refinement on	F^2	F^2	F^2	F^2
$R[F^2 > 2\sigma(F^2)]$, $wR(F^2)$, S	0.040, 0.109, 1.06	0.031, 0.069, 1.04	0.064, 0.159, 1.02	0.037, 0.101, 1.03
No. of reflections	5463	10 301	15 437	5174
No. of parameters	338	648	980	348
H-atom treatment	Mixture‡	Mixture‡	Mixture‡	Mixture‡
Weighting scheme	$w = 1/[\sigma^2(F_o^2) + (0.0591P)^2 + 0.0953P]$, where $P = (F_o^2 + 2F_c^2)/3$	$w = 1/[\sigma^2(F_o^2) + (0.0249P)^2 + 2.8514P]$, where $P = (F_o^2 + 2F_c^2)/3$	$w = 1/[\sigma^2(F_o^2) + (0.0579P)^2 + 6.1685P]$, where $P = (F_o^2 + 2F_c^2)/3$	$w = 1/[\sigma^2(F_o^2) + (0.0536P)^2]$, where $P = (F_o^2 + 2F_c^2)/3$
$(\Delta/\sigma)_{max}$	< 0.0001	0.002	0.001	< 0.0001
$\Delta\rho_{max}$, $\Delta\rho_{min}$ (e Å^{-3})	0.86, −0.53	0.58, −0.41	2.08, −0.74	0.71, −0.51
Extinction method	None	*SHELXL*	None	None
Extinction coefficient	–	0.00036 (6)	–	–
Absolute structure	–	Flack (1983)	–	–
Flack parameter	–	−0.002 (7)	–	–

	(4)	(5)	(6)
Crystal data			
Chemical formula	$C_{10}H_{20}O_5{\cdot}H_8N_2NiO_{10}{\cdot}C_{10}H_{20}O_5{\cdot}H_8N_2NiO_{10}$	$C_{10}H_{20}O_5{\cdot}C_2H_7N_3NiO_8{\cdot}C_2H_3N$	$C_{10}H_{24}O_7Ni^{2+}{\cdot}2NO_3^{1-}$
M_r	950.11	521.13	439.02
Cell setting, space group	Orthorhombic, $Pbca$	Triclinic, $P\overline{1}$	Monoclinic, $P2_1/c$
Temperature (K)	90.0 (2)	90.0 (2)	90.0 (2)
a, b, c (Å)	15.352 (1), 16.278 (1), 30.716 (2)	12.144 (1), 12.137 (1), 16.039 (1)	14.676 (1), 13.961 (1), 25.552 (2)
α, β, γ (°)	90.00, 90.00, 90.00	90.12 (1), 105.47 (1), 90.04 (1)	90.00, 96.56 (1), 90.00
V (Å^3)	7675.9 (8)	2278.4 (3)	5201.1 (7)
Z	8	4	12
D_x (Mg m^{-3})	1.644	1.519	1.682
Radiation type	Mo $K\alpha$	Mo $K\alpha$	Mo $K\alpha$
μ (mm^{-1})	1.09	0.92	1.19
Crystal form, color	Plate, pale green	Parallelepiped, pale green	Block, pale yellow
Crystal size (mm)	0.50 × 0.40 × 0.05	0.20 × 0.10 × 0.08	0.40 × 0.15 × 0.10
Data collection			
Diffractometer	Nonius KappaCCD	Nonius KappaCCD	Nonius KappaCCD

Table 2 (continued)

	(4)	(5)	(6)
Data collection method	ω scans at fixed $\chi = 55^\circ$	ω scans at fixed $\chi = 55^\circ$	ω scans at fixed $\chi = 55^\circ$
Absorption correction	Multi-scan†	Multi-scan†	Multi-scan†
T_{min}	0.612	0.837	0.647
T_{max}	0.948	0.930	0.890
No. of measured, independent and observed reflections	49 902, 8782, 6081	46 412, 10 381, 7375	75 461, 11 918, 6757
Criterion for observed reflections	$I > 2\sigma(I)$	$I > 2\sigma(I)$	$I > 2\sigma(I)$
R_{int}	0.066	0.054	0.068
θ_{max} (°)	27.5	27.5	27.5
Refinement			
Refinement on	F^2	F^2	F^2
$R[F^2 > 2\sigma(F^2)]$, $wR(F^2)$, S	0.036, 0.079, 1.02	0.043, 0.095, 1.00	0.039, 0.102, 0.96
No. of reflections	8782	10 381	11 918
No. of parameters	553	606	751
H-atom treatment	Mixture‡	Mixture‡	Mixture‡
Weighting scheme	$w = 1/[\sigma^2(F_o^2) + (0.0319P)^2 + 1.905P]$, where $P = (F_o^2 + 2F_c^2)/3$	$w = 1/[\sigma^2(F_o^2) + (0.0395P)^2]$, where $P = (F_o^2 + 2F_c^2)/3$	$w = 1/[\sigma^2(F_o^2) + (0.0457P)^2]$, where $P = (F_o^2 + 2F_c^2)/3$
$(\Delta/\sigma)_{max}$	0.001	0.001	0.002
$\Delta\rho_{max}$, $\Delta\rho_{min}$ (e Å^{-3})	0.33, −0.49	0.77, −0.57	0.42, −0.56
Extinction method	None	None	None

Computer programs used: *COLLECT* (Nonius, 1999), *DENZO-SMN* (Otwinowski & Minor, 2006), *SHELXS*97 (Sheldrick, 2008), *SHELXL*97 (Sheldrick, 2008), *XP* in *SHELXTL* (Sheldrick, 2008), *SHELX*97 and local procedures. † Based on symmetry-related measurements. ‡ Mixture of independent and constrained refinement.

monohydrate (2*a*) and sometimes of the *cis*/*trans* compound (4) rather than of the acetonitrile compound.

2.1.6. $[Ni(H_2O)_2(15\text{-crown-5})](NO_3)_2$ [the target compound, (6), diaqua(15-crown-5)nickel(II) nitrate]. Yellow crystals of the desired compound were finally obtained by heating the solid $[Ni(H_2O)_6](NO_3)_2{\cdot}(15C5){\cdot}2H_2O$ (1) to 373 K at *ca* 1−5 K min^{-1}, holding the resulting mixture of yellow solid and a small amount of solution at that temperature for 5–10 min, and then cooling to room temperature over a period of *ca* 30 min. Later experiments suggested that heating to over 350 K would have been sufficient.

2.2. Hot-stage microscopy

As the target compound (6) was produced by heating the dihydrate (1), several crystals of (1) were heated on an *Olympus BX*51 research microscope equipped with an STC200 temperature controller (*Instec*) and an *Insight Firewire 4 MegaSample Colour Mosaic* digital camera operating under the program *SPOT Advanced*4.6 (Diagnostic Instruments Inc.). The accuracy of the temperatures is ± 0.1 K. Photographs were taken about once per minute. Two sequences of images for the range 298–373 K have been archived with the supplementary material; the first sequence was taken while heating at 5 K min^{-1} and the second while heating at 1 K min^{-1}. Selected pictures from the 1 K min^{-1} sequence are shown in Figs. S-4 and S-5 of the supplementary material.

2.3. Differential scanning calorimetry (DSC)

The thermal behavior of the dihydrate (1) was also investigated by using the DSC 822^e apparatus from Mettler Toledo under the control of the software *STARe* (Version 8.10). The DSC samples were prepared from fine powders. Two samples (several mg in a pierced Al pan) were heated and cooled at a rate of 5 K min^{-1}.

The first sample was heated, then cooled, then reheated over the range 298–373 K. The second sample was first heated to only 348 K [where compound (2*b*) should be stable], then cooled to 298 K, reheated to 373 K [to make compound (6)], cooled to 298 K and finally heated once again to 373 K. Samples were held for 10 min at the maximum or minimum temperature before the direction of the temperature change was reversed. The traces are available as Figs. S-6 and S-7 of the supplementary material. Subsequent heating and cooling cycles may not be strictly comparable because of the continuing loss of water from the pierced pans, but we do not believe this loss to have been important enough to affect the conclusions drawn.

2.4. Structure determinations

All X-ray data were collected at 90 K with a Nonius KappaCCD diffractometer equipped with a CRYOCOOL-LN2 low-temperature system (CRYO Industries of America, Manchester, NH). Mo $K\alpha$ radiation from a fine-focus sealed tube was used. In all cases the data in the unintegrated frames were transformed to give reconstructed slices $nk\ell$, $hn\ell$ and hkn, n = 0–3, of the reciprocal lattice. Careful examinations of these slices showed that the crystals (except for the second polymorph of the monohydrate; see below) were phase pure. No sign of twinning was found except as described below.

During the final refinements the H atoms of the 15C5 molecules were placed at calculated positions [instruction *AFIX*23 in *SHELXL*97 (Sheldrick, 2008)] with isotropic displacement parameters having values $1.2U_{eq}$ of the attached C atom. The H atoms of coordinated waters were located in difference-Fourier maps and restrained such that the O—H

distances and H—O—H angles had values within accepted ranges [d(O—H) = 0.82–0.84 Å, d(H···H) $\simeq$ 1.30 Å so that H—O—H $\simeq$ 104.5°]. The atom-numbering schemes (see Figs. S8–S14 of the supplementary material) were made as consistent as possible; atoms O6 and O7 always belong to the axial aqua ligands that are found in all structures.

Information about the structure determinations can be found in Table 2 and the supplementary material. The estimated errors in the unit-cell constants were obtained by multiplying the values given by the software by at least a factor of 3 for the cell constants and by at least a factor of 15 for the cell angles. These factors were used in order to take into account the errors in the unit-cell constants from one crystal to another (Herbstein, 2000). A few additional details are given below. Drawings of the structures are shown in Figs. 1–6. Ellipsoid plots for all structures are included with the supplementary material (Figs. S-8–S14).

2.4.1. The dihydrate (1). Crystals studied at *ca* 290–293 K usually have the space group $P2_1/m$ with $Z' = \frac{1}{2}$ and minor disorder of the 15C5 rings. There is a transition at *ca* 295 K to a more disordered phase. If crystals grown at room temperature are flash-cooled to 90 K a modulated $P2_1$ phase with $Z' = 7$ is found. Slower cooling (*e.g.* −2 K min^{-1}) yields the $P2_1/c$, $Z' = 1$ phase (XEMGIF) described previously by Steed *et al.* (2001) at 173 K and reported here at 90 K. Structures of the other phases will be reported later (Siegler, Hao *et al.*, 2008*b*).

2.4.2. First polymorph of the monohydrate (2*a*). At *ca* 295 K the space group is $P2_1$ with $Z' = 1$ and disorder of the molecule of hydration (Siegler, Parkin & Brock, 2008). There is a phase transition at *ca* 190 K below which the space group is $P2_1$ with $Z' = 2$. The disorder of the water molecule is reduced below the phase transition, but is still present. The disorder found at 90 K is shown in the ellipsoid plot in Fig. S-9 of the supplementary material.

The conventional space group $P2_1$ of the low-temperature structure was changed to $B2_1$ to facilitate comparisons with the room-temperature structure, in which the hydrogen-bonded stacks of alternating $[Ni(H_2O)_6]^{2+}$ ions and 15C5 molecules run along the **a** axis. The transformation matrix that relates the non-standard and conventional cells is

$$\mathbf{a}(B2_1) = (101/0\bar{1}0/10\bar{1})\mathbf{a}(P2_1). \quad (1)$$

The cell constants of the $P2_1$ cell at 90 K are a = 10.220 (1), b = 16.514 (2), c = 13.644 (2) Å, and β = 95.96 (1)°.

2.4.3. Second polymorph of the monohydrate (2*b*). The conventional triclinic cell was transformed so that hydrogen-bonded stacks formed by the $[Ni(H_2O)_6]^{2+}$ ions and the 15C5 molecules are along the **a** axis rather than along [$\bar{1}$10]. This transformation facilitates comparisons with the other structures. The transformation matrix is given by

$$\mathbf{a}(P\bar{1})' = (\bar{1}10/001/100)\mathbf{a}(P\bar{1}). \quad (2)$$

The cell constants of the conventional cell at 90 K are: a = 10.163 (1), b = 13.607 (1), c = 24.765 (2) Å, and α = 82.21 (1), β = 89.71 (1), γ = 83.50 (1)°.

The refinement was not completely satisfactory. Although the R factors were not unusually high (see Table 2), the final difference-Fourier map showed peaks as large as 2.1 e Å^{-3}. The largest peaks (0.6–2.1 e Å^{-3}) were located at *ca* 1 Å from the Ni^{2+} ions. One isolated peak (1.4 e Å^{-3}) was located at *ca* 2.5 Å from one O atom of two nitrate ions and at *ca* 2.6 Å from one O atom of one $[Ni(H_2O)_6]^{2+}$ cation. Careful examination of the reconstructed reciprocal lattice slices showed the presence of some extra (*i.e.* unindexed) reflections. Since we could identify no twin law by inspection or by using the program suite *PLATON* (Spek, 2003), we believe that the refinement problems result from the presence of a second phase. This explanation is consistent with the quality of the crystals obtained. The crystallographic problems notwithstanding, we believe the overall structure to be basically correct. Disorder of one nitrate ion is observed; the occupancy factor for the major component is 0.529 (6). The displacement ellipsoids (see Fig. S-10 of the supplementary material) show no unusual features.

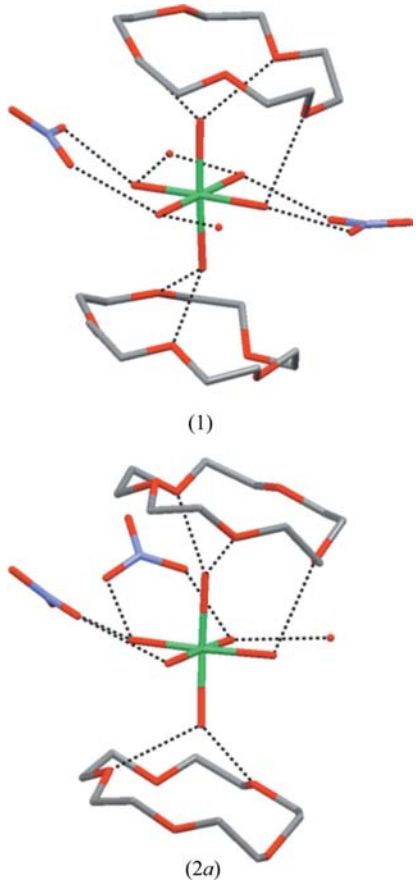

Figure 1
Diagrams showing the hydrogen-bonding motif in the dihydrate (1) and the first polymorph of the monohydrate (2*a*). For (1) the asymmetric unit is shown as well as a second crown molecule related by the *c* glide. For (2*a*), which is a modulated superstructure, the two independent crown molecules are related by an approximate translation. For (2*a*) only half of the independent cations, anions and water molecule of hydration are shown, and the disorder of the water molecule has been removed. The hydrogen bonds shown all involve the central cation, but even some of these have been removed for (2*a*) to clarify the drawing. Each coordinated water molecule makes two hydrogen bonds.

The number of formula units in the asymmetric unit (*i.e.* the number Z') is 3, but there are four independent $[Ni(H_2O)_6]^{2+}$ ions because two are located on sites of inversion symmetry.

2.4.4. The methanol compound (3). The conventional space group $P2_1/c$ was changed to $P2_1/n$ so that the hydrogen-bonded stacks of $[Ni(H_2O)_6]^{2+}$ and $[Ni(H_2O)_4(MeOH)_2]^{2+}$ ions and 15C5 molecules run along a crystallographic axis (*i.e.* **a**), as they do in other structures, rather than along [101]. The transformation matrix is given by

$$\mathbf{a}(P2_1/n) = (\bar{1}0\bar{1}/010/100)\mathbf{a}(P2_1/c). \quad (3)$$

The cell constants of the $P2_1/c$ cell at 90 K are: a = 10.429 (1), b = 15.481 (1), c = 14.118 (1) Å, β = 98.66 (1)°.

The value of Z' for this structure is $\frac{1}{2}$; each of the two cations lies on an inversion center while the one independent 15C5 molecule and the two independent nitrate ions lie on general positions. There is an up/down disorder of one CH_2OCH_2-CH_2OCH_2 section of the crown molecule (atoms O1, O2, C3, C2, C1 and C10; see Fig. S-11 of the supplementary material). In this region of the molecule strong restaints had to be applied to the bond lengths and angles and the displacement parameters of the split C atoms had to be held equal. The occupancy factor for the major component is 0.575 (3).

2.4.5. The *cis*/*trans* compound (4). There is one *cis* and one *trans* cation in the asymmetric unit. There is no imposed symmetry.

2.4.6. The acetonitrile compound (5). Crystals studied at *ca* 290–295 K have the space group $P2_1/m$ with $Z' = \frac{1}{2}$; the 15C5 ring is partially disordered by the imposed mirror symmetry. If crystals grown at room temperature are flash-cooled to 90 K a modulated $P2_1$ phase with $Z' = 5$ is found. Slower cooling (*e.g.* −2 K min^{-1}) to 90 K yields the $P\bar{1}$, $Z' = 2$ phase reported here. The α and γ angles of this cell are 90.12 (1) and 90.04 (1)° so that the pseudomerohedral twinning identified by *PLATON* (Spek, 2003) is no surprise. The twin matrix is $(\bar{1}00/010/00\bar{1})$; it corresponds to a twofold axis along the **b** axis.

The structures of the three phases stable at higher temperatures will be reported in the following publication (Siegler, Parkin & Brock, 2008).

2.4.7. The target compound (6). This compound is isostructural with the low-temperature phases of $[M(H_2O)_2(15C5)](NO_3)_2$, M = Mg, Mn, Fe and Zn (Hao, Parkin & Brock, 2005; Hao, Siegler *et al.*, 2005). This phase is a commensurately modulated superstructure; the modulation is threefold along the **c** direction.

The initial refinements showed elongated ellipsoids for the Ni ion of each cation. The ellipsoids for the axial water O atoms were somewhat elongated in the same direction, but were less eccentric (see Fig. 6). In the final least-squares cycles each of the three independent Ni ions was split over two sites [occupancy factors 0.667 (6), 0.565 (4), 0.598 (5) for the major

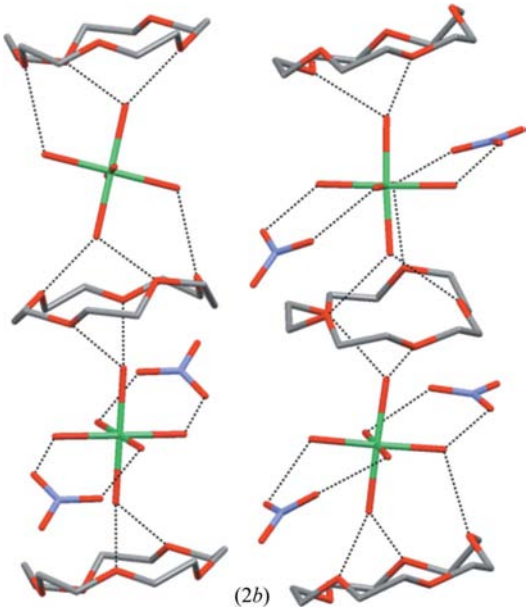

Figure 2
Diagram showing the stack motif in the second polymorph of the monohydrate (2*b*). The cations in the stack on the right lie on inversion centers; the three crown molecules in that stack are symmetry related (inversion or translation operations). The top and bottom crown molecules in the stack on the left are related by translation, but are not related to the crown in the middle. The water molecules of solvation and the one nitrate ion that does not form hydrogen bonds to two *cis* aqua ligands have been omitted. The hydrogen bonds shown all involve a central cation but some of those have been removed to clarify the drawing. All but one coordinated water molecules make two hydrogen bonds; the exception is an equatorial aqua ligand in the molecule in the lower right. Note the differences in the hydrogen-bonding patterns in the two stacks. Both cations in the stack on the right form hydrogen bonds to two bridging nitrate ions; in the stack on the left one cation does but the other does not. In the stack on the right each cation has one equatorial aqua ligand that forms an O—H···O bond to an adjacent crown. In the stack on the left one cation has two equatorial aqua ligands that form such bonds, while the other cation forms no such O—H···O bond.

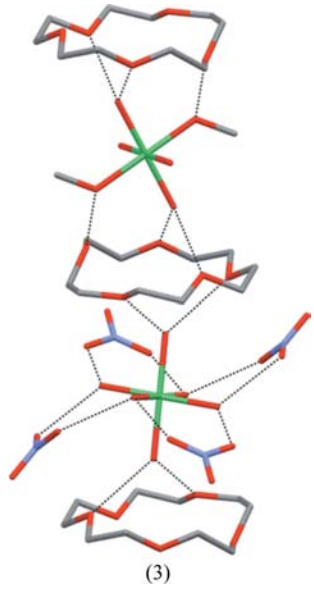

Figure 3
Diagram showing the stack motif in the methanol compound (3). The two cations lie on inversion centers so that all three crown molecules are related by symmetry; the top and bottom crown are related by translation. Two of the four nitrate ions shown are independent. The O—H···O bonds involving the two equatorial aqua ligands of the upper cation have been omitted for the sake of clarity. Each coordinated water molecule makes two hydrogen bonds. The minor component of the disordered crown ether has been omitted for clarity.

components]. The two partial-occupancy Ni ions in each cation are close enough together [0.420 (3), 0.423 (2) and 0.413 (3) Å] that the displacement ellipsoids for the members of each pair had to be constrained to be the same (EADP instruction; Sheldrick, 2008). Inclusion of a disorder model for the Ni^{2+} ions (see Fig. 6) improved the model significantly: the R_1 value dropped from 0.049 to 0.039, the highest residual electron-density peak dropped from 0.95 e $Å^{-3}$ to 0.42 e $Å^{-1}$, and the ellipsoids became much less eccentric. The final model includes ordered O_{water} atoms with rather large displacement ellipsoids because including disorder in the model did not improve the refinement significantly.

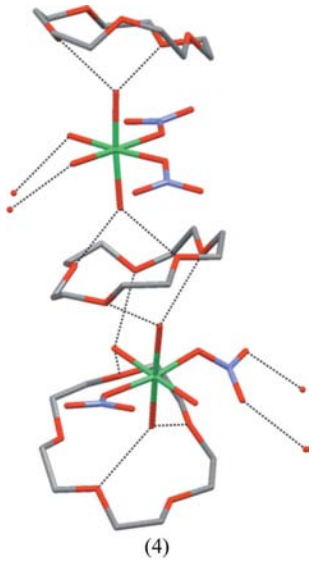

Figure 4
Diagram showing the stack motif in the *cis*/*trans* compound (4). The drawing shows the asymmetric unit plus one additional crown molecule; the crowns at the top and bottom of the drawing are related by the *c* glide. Most O—H···O bonds between stacks have been left out to improve clarity, but each coordinated water molecule makes two hydrogen bonds. The interaction in which a nitrato ligand on the *trans* cation forms O—H···O bonds with the two equatorial aqua ligands in the *cis* cation is illustrated.

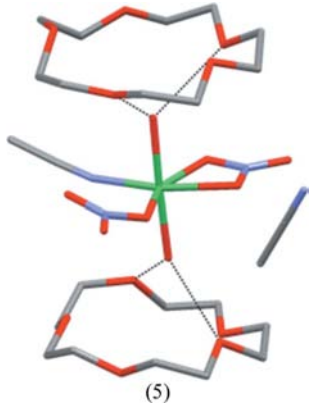

Figure 5
Diagram showing the stack motif in the acetonitrile compound (5). Only one of the two independent cations and one of the acetonitrile solvent molecules are shown; the second set is related to the first by an approximate glide plane that includes the stack axis and the acetonitrile ligand. There are only four O—H···O bonds per cation, but an uncoordinated MeCN molecule has two important C—H···O contacts to nitrate O atoms and the MeCN ligand has one important C—H···N contact to the free MeCN. These contacts are more than 0.2 Å shorter than the sum of the van der Waals radii (Bondi, 1964).

3. Results

3.1. Compositional differences

The initial strategies used to reduce the ratio of H_2O to Ni^{2+} (see Table 1) were successful, even though they did not produce the target compound (6). In the dihydrate (1) and monohydrates (2*a*) and (2*b*), the Ni^{2+} ions are octahedrally coordinated by six water molecules. In the methanol compound (3) two *trans* aqua ligands in one of the two independent cations are replaced by two methanol ligands. In the *cis*/*trans* compound (4) two nitrate counterions become monodentate nitrato ligands and replace two of the equatorial aqua ligands. In the acetonitrile compound (5) one of the two nitrato ligands becomes bidentate and replaces the third equatorial aqua ligand, and a MeCN ligand replaces the fourth (see Fig. 5).

3.2. Common structural features

The Ni^{2+} ions in all structures are coordinated by two water molecules that are in the *trans* orientation; these aqua ligands will be described as axial. Each of the axial aqua ligands is the donor in two O—H···O bonds to the co-crystallized 15-crown-5 molecules.[2]

Stacks of alternating $(H_2O)_{ax}$–NiL_4–$(OH_2)_{ax}$ units and 15C5 molecules are found in all structures except that of the target compound (see Figs. 1–5). Each axial aqua ligand forms two O—H···O bonds to nonadjacent O atoms in the nearest crown molecule. The axial aqua ligand on the other side of the crown does the same. The fifth O atom of the crown ether is the acceptor of an O—H···O bond from one of the equatorial ligands (aqua or methanol), except in the acetonitrile structure (5) in which there is no available equatorial H atom. The $(H_2O)_{ax}$–NiL_4–$(OH_2)_{ax}$ stacks are crosslinked by O—H···O bonds from water molecules to nitrate ions or waters of hydration. The spacing along the stack axis for (1), (2*a*), (2*b*), (3) and (5) varies from 7.99 to 8.05 Å. In (4) the spacing is a little smaller (7.68 Å) because the stacks 'wave' (see Fig. 4) to accommodate the one equatorial aqua ligand that makes O—H···O bonds to both adjacent crowns.

Views down the stack axes are shown in Fig. 7.

A common motif in these structures is the formation by two adjacent equatorial aqua ligands of O—H···O bonds to a single nitrate ion that bridges the two water ligands. In the dihydrate (1) each cation forms two such bridges, which can be described as *trans* (see Fig. 1). In the first monohydrate polymorph [(2*a*), Fig. 1] there are also two bridges, but one equatorial aqua ligand is a donor for both so that the bridges can be said to be *cis*. The *trans* version of the motif occurs for

[2] The existence of O—H···O bonds has been inferred from O···O distances shorter than 3.00 Å and the availability of an H atom. In most cases the positions of the participating H atoms are known at least approximately.

three of the four independent cations in the second monohydrate polymorph (2*b*), but does not occur at all for the fourth cation (see Fig. 2). In the methanol compound (3) this motif occurs four times for the $[Ni(H_2O)_6]^{2+}$ cation (see Fig. 3), but not at all for the $[Ni(H_2O)_4(MeOH)_2]^{2+}$ cation because the protons of the equatorial MeOH ligands both interact with adjacent crowns. In the *cis*/*trans* compound (4) the two aqua ligands of the *cis* cation are bridged by the two available O atoms of one of the nitrato ligands of the *trans* cation (see Fig. 4). This bridging motif is clearly important. The motif also occurs four times in the simpler salt $[Ni(H_2O)_6](NO_3)_2$ (Bigoli *et al.*, 1971).

3.3. Ni—O_{aq} bond lengths

The mean Ni—O_{ax} bond length for the eight hexaaqua cations is 2.037 (3) Å. The one unique Ni—O_{ax} bond length in the $[Ni(H_2O)_4(MeOH)_2]^{2+}$ cation [(3), 2.049 (2) Å] is marginally longer, but then so is the unique Ni—O_{ax} distance [2.052 (2) Å] in the hexaaqua ion of that same crystal. The Ni—O_{ax} distance [2.020 (3) Å] in the acetonitrile cation (5) is a little shorter. The average Ni—O_{ax} distance in the target compound (6) is shorter yet [1.990 (3) Å].

The range of Ni—O_{ax} distances within a structure is always less than 0.015 Å, except for the second monohydrate polymorph (2*b*), where it is 0.031 Å, and the *cis*/*trans* compound (4), where it is 0.023 Å. In structure (2*b*) the four independent cations have the same composition, and in structure (4) the *cis* and *trans* isomers have nearly the same average Ni—O_{ax} distance. It therefore seems likely that the relatively large spread of the Ni—O_{ax} distances in (2*b*) and (4) results from the significant differences between the environments of the several cations in the asymmetric units.

The Ni—O_{eq} distances in the eight hexaaqua cations average 2.050 (3) Å. The range of Ni—O_{eq} distances is largest for the second polymorph of the monohydrate, where it is 0.048 Å. Again, this range probably results from the difference in environments of the four independent cations. The range is also large (0.037 Å) for the $[Ni(H_2O)_4(MeOH)_2]^{2+}$ cation, but in that case the difference is between two chemically different bonds: a short Ni—OH_2 bond [2.022 (2) Å] and a longer Ni—O(H)Me bond [2.059 (2) Å].

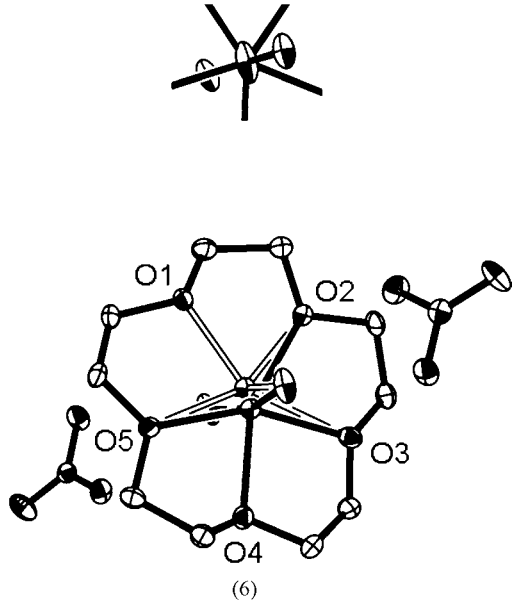

(6)

Figure 6
Ellipsoid plot (50% probability level) for one of the formula units of the target compound (6) at 90 K. When the Ni^{2+} ion is treated as ordered (upper drawing, which shows the Ni^{2+} ion and axial aqua ligands only) its ellipsoid is large and eccentric. The split-atom model (lower drawing) for the Ni^{2+} ion is more satisfactory. The ellipsoid plots for the other two sets of ions in the asymmetric unit are very similar. The atom-numbering scheme for all three cations is the same.

3.4. $O_{ax}\cdots O_{crown}$ distances

The 44 $O_{ax}\cdots O_{crown}$ distances found in the six structures containing the 15 C5$\cdots H_2O-M-OH_2\cdots$15C5 motif are in the range 2.675–2.876 Å; the spread is therefore 0.201 Å (most individual s.u.s are 0.002 Å, but a few are as large as 0.005 Å). The ranges for the individual structures are all at least 0.15 Å, except for the dihydrate [(1), 0.08 Å] and the methanol compound [(3), 0.09 Å].

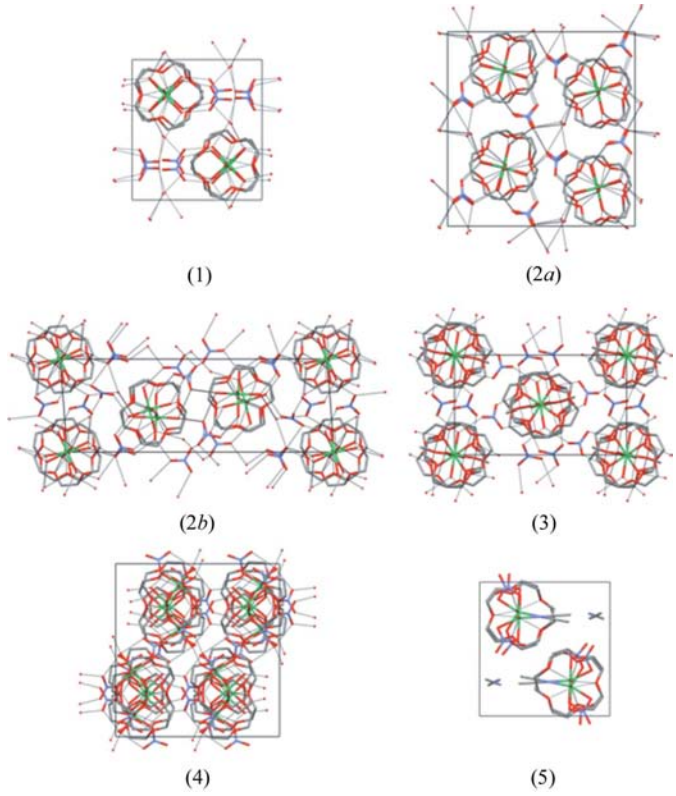

Figure 7
Projections down the stack axes for structures (1)–(5). The O—H$\cdots$O bonds drawn by the program *MERCURY* (Macrae *et al.*, 2006) using the default definition are shown. The motifs in which a pair of *cis* aqua ligands form O—H$\cdots$O bonds to a bridging nitrate ion can be seen. The complexity of the second polymorph of the monohydrate (2*b*) is noteworthy as is the similarity of the dihydrate (1) and the acetonitrile compound (5). The stacks in the *cis*/*trans* compound (4) are less straight than in the other structures.

3.5. Ni—O_{crown} bond lengths in the target compound (6)

Each of the three independent Ni^{2+} ions has one Ni—O distance in the range 2.0–2.1 Å, two Ni—O distances in the range 2.1–2.2 Å, one Ni—O distance in the range 2.25–2.35 Å and one Ni—O distance in the range 2.49–2.55 Å (atom O1 or O4). In the structural model that does not include disorder the Ni ellipsoids are longest in the direction of the longest bonds (see Fig. 6). It seems that the Ni^{2+} ion is only coordinated strongly by four (or perhaps by only three) of the five ether O atoms, and is disordered because there are two possible positions that correspond to nearly the same positions for the axial O atoms, whose positions are restricted by the overall hydrogen-bond pattern.

This pattern of Ni—O bond lengths is similar to those seen in two other pentagonal bipyramidal complexes of Ni^{2+} (Giordano *et al.*, 1979; Pelizzi *et al.*, 1986) that have axial aqua ligands. In these two complexes, however, three of the coordinating atoms in the equatorial plane are N rather than O atoms so that the exact distances cannot be compared.

3.6. Thermal studies of the dihydrate (1)

Since heating the dihydrate (1) led to the insertion of the Ni^{2+} ion into the crown ligand it is important to understand the behavior of the dihydrate crystals during heating.

Hot-stage microscopy at 5 K min^{-1} shows melting at 342–344 K. At 1 K min^{-1} the melting takes place (as expected) at a slightly lower temperature (339–341 K) and is seen to be incongruent (melting with immediate nucleation of a new solid phase that exists in contact with a liquid). The DSC scans (two powder samples) also show an important endotherm at 339–340 K.

The second polymorph of the monohydrate (2*b*) is formed, as shown by the structure determination of (2*b*), if the dihydrate is heated to only 348 K before cooling. This observation is consistent with the slower hot-stage microscopy run, which shows the nucleation of crystals of a new phase at *ca* 341 K with melting to give a second new phase [the target compound, (6)] just above 350 K. We believe that the second polymorph (2*b*) of the monohydrate exists in contact with a small amount of solution in the range 340–349 K.

The phase that nucleates above 350 K continues to grow until *ca* 370 K (perhaps because of continued evaporation of water) and is clearly yellow. The yellow color is a strong indication that the new phase contains the $[Ni(H_2O)_2(15C5)]^{2+}$ cation. This interpretation is supported by the structure determination of (6). When the heating rate was 5 K min^{-1} this yellow phase nucleated at 358 K rather than 350 K, presumably because of kinetic factors.

The first DSC heating runs (5 K min^{-1}) showed no feature between 348 and *ca* 363 K, where there was a weak, and very wide, endotherm. We believe this endotherm corresponds to the formation of the target compound, which nucleated at 358 K in the hot-stage microscopy run when the heating rate was 5 K min^{-1}. The endotherm is sufficiently wide that its onset temperature is uncertain by at least 5 K.

The second DSC sample was first heated to only 348 K, at which temperature the second monoclinic polymorph only should have been present and there was little likelihood of much $[Ni(H_2O)_2(15C5)](NO_3)_2$ having been formed. When this sample was cooled the first exotherm appeared at 317 K. The first exotherm for samples that had previously been heated to 373 K is at 311–313 K.

The second heating run for a sample first heated to only 348 K looks like the first, but additional peaks are present if the sample has been previously heated to 373 K. These observations are consistent with a change in the identity of the compound above 350 K.

The phase present below 311–313 K in samples of the dihydrate (1) that have first been heated to 373 K is the triclinic form of the target compound (6). The triclinic phase transforms to the $P2_1/c$, $Z' = 3$ phase reported here at *ca* 284 K (Siegler, Hao *et al.*, 2008*b*) in a transformation that leaves single crystals intact.

Finally, we note that the 1 K min^{-1} microscopy run shows obvious evidence of a solid–solid phase transition starting at *ca* 320 K and continuing until the melting at 340 K (see Fig. S-5 of the supplementary material). Crystallites of the new phase can be seen growing inside the original crystal. The faces of the new crystallites appear to be quite well aligned with each other. There is no evidence of this transition in the DSC curve. We were unable to determine the structure of this phase.

4. Discussion

4.1. Why is it so difficult to get the Ni^{2+} ion into the crown?

We surmise, from the many reported structures containing Ni^{2+} and crown ligands, that a number of research groups have tried to make the $[Ni(H_2O)_2(15C5)]^{2+}$ complex. There are, however, only two entries in the CSD that indicate a nickel atom or ion inside any crown ligand.

The entry for the compound $[Ni(EtOH)_3(18\text{-crown-}6)](PF_6)_2$ (BIXXAH10; Larson *et al.*, 1989) includes coordinates. The Ni^{2+} ion is coordinated to three of six O atoms of the crown and to three ethanol molecules. The original reference shows that the compound was synthesized with methods aimed at excluding water. The second entry, for $[Ni(EtOH)_2(15C5)](PF_6)_2$ (BIHFED), does not include coordinates, but the referenced conference abstract (Simonsen *et al.*, 1982) suggests that the Ni^{2+} ion has four shorter and one longer interaction with the O atoms and that the crown ligand is disordered.

4.1.1. Ion size. The ions $[M(H_2O)_6]^{2+}$ have high-spin configurations; replacement of four water molecules by the 15C5, which coordinates more weakly than water, will not change the spin. Of all the M^{2+} ions investigated, Ni^{2+} has the second smallest high-spin radius (Greenwood & Earnshaw, 1997; see Table 3) and so fits poorly in the crown. The only smaller M^{2+} ion is Mn^{2+}, which has a high-spin d^5 electronic configuration. It therefore imposes no geometrical preference on its environment and the metal ion can reside in a 'compromise' position near the center of the 15C5 equatorial

Table 3
Properties of some M^{2+} ions.

Ion	Configuration	Ionic radius (Å)†	Octahedral CFSE	Hydration enthalpy (kJ mol^{-1} × 10^{-3} or MJ)	log(k_{H2O})‡ (s^{-1})
Mg^{2+}	d^0	0.72	0 Δ_o	−1.98[a]	5.0[b]
Mn^{2+}	d^5	0.67	0 Δ_o	−2.74[c]	7.32[d]
Fe^{2+}	d^6	0.78	0.4 Δ_o	−2.85 [c]	6.64[d]
Co^{2+}	d^7	0.745	0.8 Δ_o	−2.92 [c]	6.51[d]
Ni^{2+}	d^8	0.69	1.2 Δ_o	−3.00 [c]	4.50[d]
Cu^{2+}	d^9	0.73	0.6 Δ_o	−3.00 [c]	9.9[d]
Zn^{2+}	d^{10}	0.74	0 Δ_o	−2.94 [c]	7.5[d]

References: (*a*) Noyes (1962); (*b*) Eigen (1963); (*c*) George & McClure (1959); (*d*) Tobe (1987). † Six-coordinate radius; high-spin for Fe^{2+} and Co^{2+} (Greenwood & Earnshaw, 1997, pp. 111, 1043, 1074, 1115, 1148, 1176, 1205). ‡ Self-exchange rate constant for $[M(H_2O)_6]^{2+}$ with H_2O at 298 K.

ligand. In contrast, the high-spin, d^8 Ni^{2+} ion has a stereochemical preference for octahedral geometry (*see below*), leading it to approach an octahedron as closely as its small size allows. This conclusion is consistent with the structures of BIXXAH10, BIHFED and (6), in which the Ni^{2+} ion is substantially closer to some O_{crown} atoms than to others.

4.1.2. Energies of *d* orbitals. The octahedral crystal-field stabilization energy (CFSE) for a d^8 system is greater than for d^n ions with n = 0 or 5–10 (see Table 3). Furthermore, the energy of high-spin d^8 Ni^{2+} is unaffected by a Jahn–Teller distortion because the number of electrons in the e_g orbitals is even and the distortion cannot change the overall spin. The energy lowering that results from a Jahn–Teller distortion when the number of electrons in the e_g orbitals is odd (as in d^7 Co^{2+} and d^9 Cu^{2+}) is not found for Ni^{2+}.

The small size of the Ni^{2+} ion also leads to one of the most favorable hydration energies of those ions being considered (Noyes, 1962; George & McClure, 1959; see Table 3). Furthermore, the small size and large octahedral CFSE of Ni^{2+} lead to slow ligand exchange of $[Ni(H_2O)_6]^{2+}$ in aqueous solution. The self-exchange of $[M(H_2O)_6]^{2+}$ with water is *ca* 1000 times slower for Ni^{2+} than for the other divalent ions from Mn^{2+} to Zn^{2+}, and *ca* 10 times slower for Ni^{2+} than for Mg^{2+} (Eigen, 1963; Tobe, 1987; see Table 3). As a result, it is both thermodynamically and kinetically difficult for $[Ni(H_2O)_6]^{2+}$ to exchange its strongly bonded water ligands for a more weakly bonding and less symmetrical 15-crown-5 ligand.

4.2. Entropy considerations

In an aqueous solution of an M^{2+} ion with a weakly coordinating anion (such as NO_3^- or ClO_4^-) the metal is hydrated to give $[M(H_2O)_n]^{2+}$, where n is most often 6. If 15C5 is also present the M^{2+} ion is often inserted into the crown because the reaction

$$[M(H_2O)_n]^{2+} + \text{15-crown-5} \rightarrow [M(H_2O)_2(\text{15-crown-5})]^{2+} + (n-2)H_2O$$

is entropically favorable. The entropy advantage of increasing the number of molecules by $n - 3$ allows the reaction to go forward, even though the M—O_{crown} bonds are usually weaker than the M—O_{aq} bonds. This reaction occurs at room temperature for M = Mg^{2+}, Mn^{2+}, Fe^{2+}, Co^{2+}, Cu^{2+} and Zn^{2+} (Hao, Parkin & Brock, 2005; Hao, Siegler *et al.*, 2005), but not for Ni^{2+}. Our observation that the reaction for M = Ni^{2+} takes place above 350 K is consistent with the idea that an entropy advantage offsets an energy disadvantage. The increased rate of ligand exchange at the higher temperature is probably also important in allowing the formation of $[Ni(H_2O)_2(15C5)]^{2+}$.

4.3. Why is the 15C5···H_2O—*M*—OH_2···15C5 motif so important?

The six structures (1)–(5) are all co-crystals of 15C5 and a coordinated Ni^{2+} ion. The existence of a co-crystal corresponds to a failure of fractional crystallization. The formation of a co-crystal almost always lowers the packing efficiency (see Lloyd *et al.*, 2007) and so is unlikely to occur unless there is an offsetting energy or entropy advantage. In the case of these six structures it is the formation of O—H···O bonds between the coordinated Ni^{2+} and the crown molecule that is determining. An indication of the importance of these bonds is the relatively faster crystal growth, as shown by greater crystal length, along the direction of the hydrogen-bonded chains, *i.e.* in the projection direction of the drawings in Fig. 7.

Steed *et al.* (2001) have termed the 15-crown molecule an 'unsymmetrical bifacial hydrogen-bond acceptor'. Another way of saying the same thing is to note that the crown presents a tidy package of hydrogen-bond acceptors. All the Ni^{2+} complexes (with the possible exception of the acetonitrile-containing complex) have more hydrogen-bond donors than acceptors; the hexaaqua cations have many more donors than acceptors. Co-crystallization with a molecule that is rich in hydrogen-bond acceptors and has no O—H···O bond donors is therefore easy to understand.

Since ether O atoms are weaker hydrogen-bond acceptors than water (see *e.g.* Steiner, 2001) it seems almost certain that the individual O—H···O_{crown} bonds are weaker in solution than O—H···O bonds to solvent water molecules would be. An entropy effect, however, is probably again important. If a 15C5 molecule is available one metal complex can form four (often five) O—H···O bonds to two crown molecules rather than to the larger number of water molecules that would have to be present to satisfy the same donors.

A survey of the CSD shows that the 15C5···H_2O–*M*–OH_2···15C5 motif is common. The same type of motif has also been found for Ni^{2+} complexes crystallized in the presence of 18-crown-6 [refcodes HEKDIK and HEKKOX (Steed *et al.*, 1998)] and 12-crown-4 [refcode MEYLAD (Junk *et al.*, 2001)]. Other metal ions in higher oxidation states also form such chains; a search of the CSD for structures containing 15C5, the H_2O—*M*—OH_2 fragment, and a metal oxidation state of 3 or

higher turned up 21 different structures containing the 15C5···H_2O—M—OH_2···15C5 motif. Since axial aqua ligands are always present it seems the driving force for the formation of such chains is almost certainly the formation of a tidy package of O—H···O bonds.

Problems with the packing of the pure nickel nitrate hexahydrate and pure 15C5 compounds probably also matter. In general, the formation of co-crystals is more likely if the individual components have unexpectedly low melting points, which suggest unsatisfactory packing. The melting point (330 K; Marcus *et al.*, 2005) of $[Ni(H_2O)_6](NO_3)_2$ is low for a simple ionic compound that can form O—H···O bonds. The hot-stage microscopy indicates that the dihydrate co-crystal (1) melts *ca* 10 K higher than this purely inorganic salt.

The melting point of 15C5 (239 K; Udachin & Lipkowski, 1996) is also low, probably because of its awkward shape. This temperature can be compared with the higher melting points of 18-crown-6 = 18C6 (311–313 K; Gokel *et al.*, 1988) and 12-crown-4 = 12C4 (*ca* 273 K; Groth, 1978). There are two other indications that 15C5 packs less well than 12C4 and 18C6. First, there are two independent molecules of 15C5 in its crystal ($P4_1$; Parsons, 2007), while $Z' = \frac{1}{2}$ for both 12C4 ($P\bar{1}$; Groth, 1978) and 18C6 (*Pbca*; Maverick *et al.*, 1980), in which the one independent molecule lies on an inversion center. Second, there are the packing coefficients calculated with the *CALC VOID* routine in *PLATON* (Spek, 2003) for these three structures, all of which were determined in the range 100–123 K. The values are 0.716 and 0.733 for 12C4 and 18C6, but only 0.693 for 15C5.

4.4. Why are the asymmetric units in these compounds so large?

The complexity of the structures of crystals grown from aqueous solutions of $Ni(NO_3)_2$ and 15-crown-5 is stunning. Structures with $Z' > 1$ and structures containing chemically different molecules (or ions of the same charge) are uncommon in general but seem to be the norm in this system (see Table 1). In two [(3) and (4)] of the six structures reported here that contain the 15C5···H_2O—M—OH_2···15C5 motif there are two chemically distinct cations. In another structure (2*b*) there are cations that form quite different types of hydrogen bonds. Steed *et al.* (2001) made similar observations about structural complexity for compounds containing a coordinated metal ion and the 15C5 molecule.

This system is seen to be even more complex if phase transitions are considered. Crystals of compounds (1) and (5) grown slightly above room temperature pass through three phase transitions each when cooled slowly to 90 K (Siegler, Hao *et al.*, 2008*b*; Siegler, Parkin & Brock, 2008). There is no obvious crystal damage in either case, and in both cases there is an intermediate phase with exceptionally high Z' values (7 and 5).

The compounds $[M(H_2O)_2(15C5)](NO_3)_2$, M = Mg, Mn, Fe, Co, Ni, Cu and Zn, also all undergo non-destructive phase transitions between 306 and 278 K (Hao, Siegler *et al.*, 2005; Siegler, Hao *et al.*, 2008*a*). The Z' values (2 and $\frac{1}{2}$) for the M = Co compound are not unusual, but some of the Z' values for the other compounds (2, 3, 5 and 8) are exceptional.

So why are the asymmetric units in this system so often large? A check of the most recent version of the CSD shows that 91.2% of structures have $Z' \leq 1$ and that less than 0.9% have $Z' \geq 3$, so the high-Z' structures found in this system are oddities. We have argued (Hao, Siegler *et al.*, 2005) that the large Z' values in the compounds $[M(H_2O)_2(15\ C5)](NO_3)_2$ are a consequence of a conflict between efficient packing of the 15-crown-5 ligands, which requires unequal spacing of the M^{2+} ions, and optimization of the hydrogen-bonding pattern, which would require equal spacing of the axial aqua ligands.

The reasons for the large asymmetric units in structures containing the 15C5···H_2O—M—OH_2···15C5 motif are less clear, but probably also point to packing problems. The shape of the 15C5 molecule is almost certainly a factor, as has already been suggested by Steed *et al.* (2001). The need to satisfy a rather large number of donors (aqua ligands) and acceptors (crown molecules and nitrate ions) is another. The requirement of a favorable arrangement of ionic charges [except in (5)] complicates the situation further. The fitting together in a structure of chains (or stacks if the van der Waals surfaces are considered) of relatively fixed geometry may also be a problem.

The inclusion of solvent molecules in (1), (2*a*), (2*b*) and (5) is another indication of packing difficulties.

5. Summary

The compound $[Ni(H_2O)_2(15\text{-crown-}5)](NO_3)_2$ has been prepared by heating solid $[Ni(H_2O)_6](NO_3)_2{\cdot}15C5{\cdot}2H_2O$. The resulting crystal structure is closely related to those of the series $[M(H_2O)_2(15C5)](NO_3)_2$, M = Mg, Mn, Fe, Cu and Zn. Very recent experiments (Siegler, 2008) show that the same $[Ni(H_2O)_2(15\text{-crown-}5)]^{2+}$ cation can be formed by heating when the counterion is HSO_4^-.

The Ni compound can be formed only at temperatures above *ca* 350 K because the replacement of water ligands by the crown ligand becomes more entropically favorable and kinetically feasible.

During attempts to produce the target compound by limiting the water available, five new structures containing the 15C5···H_2O—M—OH_2···15C5 motif were discovered. This motif, which requires the formation of a co-crystal, is prevalent because the 15C5 molecule can satisfy five O—H donors in a tidy way. Entropy is again a factor.

The complexity of the asymmetric units for compounds in this series is striking. Many structures have $Z' > 1$; other structures contain more components (molecules and ions) than is necessary chemically. We believe that this complexity points to crystal packing problems, which include satisfying all the donors and acceptors present, filling space efficiently and finding a favorable arrangement of any charged species present. The very approximate fivefold symmetry of the 15-crown-5 molecule may also be important.

MAS thanks the University of Kentucky for a 2006–07 Kentucky Opportunity Fellowship. We thank Professor Tonglei Li of the University of Kentucky College of Pharmacy for his help with the hot-stage microscopy, and Professor Mark D. Watson of the University of Kentucky Chemistry Department for help with the DSC measurements.

References

Allen, F. H. (2002). *Acta Cryst.* B**58**, 380–388.

Bigoli, F., Braibanti, A., Tiripicchio, A. & Camellini, M. T. (1971). *Acta Cryst.* B**27**, 1427–1434.

Bondi, A. (1964). *J. Phys. Chem.* **68**, 441–451.

Eigen, M. (1963). *Pure Appl. Chem.* **6**, 97–115.

Flack, H. D. (1983). *Acta Cryst.* A**39**, 876–881.

George, P. & McClure, D. S. (1959). *Prog. Inorg. Chem.* **1**, 381–463.

Giordano, T. J., Palenik, G. J., Palenik, R. C. & Sullivan, D. A. (1979). *Inorg. Chem.* **9**, 2445–2450.

Gokel, G. W., Cram, D. J., Liotta, C. L., Harris, H. P., Cook, F. L., Noe, E. A., Raban, M. & Johnson, C. R. (1988). *Org. Synth.* **6**, 301–303.

Greenwood, N. N. & Earnshaw, A. (1997). *Chemistry of the Elements*, 2nd ed. Oxford: Butterworth-Heinemann.

Groth, P. (1978). *Acta Chem. Scand. A*, **32**, 279–280.

Hao, X., Parkin, S. & Brock, C. P. (2005). *Acta Cryst.* B**61**, 675–688.

Hao, X., Siegler, M. A., Parkin, S. & Brock, C. P. (2005). *Cryst. Growth Des.* **5**, 2225–2232.

Herbstein, F. H. (2000). *Acta Cryst.* B**56**, 547–557.

Junk, P. C., Smith, M. K. & Steed, J. W. (2001). *Polyhedron*, **20**, 2979–2988.

Larson, S. B., Simonsen, S. H., Ramsden, J. N. & Lagowski, J. J. (1989). *Acta Cryst.* C**45**, 161–163.

Lloyd, M. A., Patterson, G. E., Simpson, G. H., Duncan, L. L., King, D. P., Fu, Y., Patrick, B. O., Parkin, S. & Brock, C. P. (2007). *Acta Cryst.* B**63**, 433–447.

Macrae, C. F., Edgington, P. R., McCabe, P., Pidcock, E., Shields, G. P., Taylor, R., Towler, M. & van de Streek, J. (2006). *J. Appl. Cryst.* **39**, 453–457.

Marcus, Y., Minevich, A. & Ben-Dor, L. (2005). *Thermochim. Acta*, **432**, 23–29.

Maverick, E., Seiler, P., Schweizer, W. B. & Dunitz, J. D. (1980). *Acta Cryst.* B**36**, 615–620.

Nonius (1999). *COLLECT*. Nonius BV, Delft, The Netherlands.

Noyes, R. M. (1962). *J. Am. Chem. Soc.* **84**, 513–522.

Otwinowski, Z. & Minor, W. (2006). *International Tables for Crystallography*, Vol. F, ch. 11.4, pp. 226–235.

Parsons, S. (2007). *Acta Cryst.* E**63**, o3130.

Pelizzi, C., Pelizzi, G., Porretta, S. & Vitali, F. (1986). *Acta Cryst.* C**42**, 1131–1133.

Sheldrick, G. M. (2008). *Acta Cryst.* A**64**, 112–122.

Shannon, R. D. (1976). *Acta Cryst.* A**32**, 751–767.

Siegler, M. A. (2007). PhD Dissertation. University of Kentucky.

Siegler, M. A. (2008). Personal communication.

Siegler, M. A., Hao, X., Parkin, S. & Brock, C. P. (2008*a*). *Acta Cryst.* B**64**, 738–749.

Siegler, M. A., Hao, X., Parkin, S. & Brock, C. P. (2008*b*). In preparation.

Siegler, M. A., Parkin, S. & Brock, C. P. (2008). In preparation.

Simonsen, S. H., Larson, S. B. & Ramsden, J. (1982). Am., Ser. 2, **10**, 37. Abstract from meeting of the American Crystallographic Association.

Spek, A. L. (2003). *J. Appl. Cryst.* **36**, 7–13.

Steed, J. W., McCool, B. J. & Junk, P. C. (1998). *J. Chem. Soc. Dalton Trans.* pp. 3417–3424.

Steed, J. W., Sakellariou, E., Junk, P. C. & Smith, M. K. (2001). *Chem. Eur. J.* **7**, 1240–1247.

Steiner, T. (2001). *Acta Cryst.* B**57**, 103–106.

Tobe, M. L. (1987). *Comprehensive Coordination Chemistry: The Synthesis, Reactions, Properties and Applications of Coordination Compounds*, edited by G. Wilkinson, R. D. Gillard & J. A. McCleverty, Vol. 1, ch. 7.1, pp. 281–329. Oxford: Pergamon Press.

Udachin, K. A. & Lipkowski, J. (1996). *Mendeleev Commun.* pp. 197–198.